adequate screening methods may grossly underestimate prevalence rates. Healthcare providers using agar-based screening methods should evaluate the benefits of using various agars including chromID CARBA SMART for their individual settings.

Conflicts of interest and sources of funding: The authors state that there are no conflicts of interest to disclose.

Siew Yong Lee[1], Sophie Octavia[2], Ka Lip Chew[1]

[1]Department of Laboratory Medicine, National University Hospital, Singapore; [2]National Public Health Laboratory, Ministry of Health, Singapore

Contact Dr Ka Lip Chew.
E-mail: ka_lip_chew@nuhs.edu.sg

1. Marimuthu K, Venkatachalam I, Xin Khong W, *et al*. Carbapenemase-Producing *Enterobacteriaceae* in Singapore (CaPES) Study Group. Clinical and molecular epidemiology of carbapenem-resistant Enterobacteriaceae among adult inpatients in Singapore. *Clin Infect Dis* 2017; 64 (Suppl 2): S68−75.
2. Vrioni G, Daniil I, Voulgari E, *et al*. Comparative evaluation of a prototype chromogenic medium (ChromID CARBA) for detecting carbapenemase-producing Enterobacteriaceae in surveillance rectal swabs. *J Clin Microbiol* 2012; 50: 1841−6.
3. Girlich D, Anglade C, Zambardi G, *et al*. Comparative evaluation of a novel chromogenic medium (chromID OXA-48) for detection of OXA-48 producing Enterobacteriaceae. *Diagn Microbiol Infect Dis* 2013; 77: 296−300.
4. Teo JWP, La MV, Lin RTP. Development and evaluation of a multiplex real-time PCR for the detection of IMP, VIM, and OXA-23 carbapenemase gene families on the BD MAX open system. *Diagn Microbiol Infect Dis* 2016; 86: 358−61.
5. Karlowsky JA, Lob SH, Kazmierczak KM, *et al*. In vitro activity of imipenem against carbapenemase-positive Enterobacteriaceae: SMART Global Surveillance Program 2008-2014. *J Clin Microbiol* 2017; 55: 1638−49.

DOI: https://doi.org/10.1016/j.pathol.2018.08.017

MMR protein immunohistochemistry and microsatellite instability in gastric cancers

Sir,

Microsatellite instability-high (MSI-H) is emerging as a new therapeutic target for cancer immunotherapy. In May 2017, the United States Food and Drug Administration (FDA) granted accelerated approval of pembrolizumab for treatment of patients with unresectable or metastatic MSI-H or mismatch repair deficient (dMMR) solid tumours.[1] MSI-H is one major molecular subtype of gastric cancer (GC)[2,3] and is associated with high expression of programmed cell death-ligand 1 (PD-L1).[1,4] Given the relatively high incidence of MSI-H GC in patients with stage III−IV GC,[5] the effective therapeutic use of anti-PD-1/PD-L1 inhibitor in MSI-H GC could contribute to remarkable improvement in survival of patients with GC.

The most accurate method for detecting MSI to date is polymerase chain reaction (PCR), which requires a long test time, is expensive, and is difficult to interpret. So, faster, cheaper, and easily accessible diagnostic algorithms are needed. To investigate how accurately MSI-H cancers can be detected by MMR protein IHC and the distributions of protein losses in dMMR GC, we performed 4 MMR protein IHC and MSI pentaplex test in 580 GC from Asian/Korean patients.

The correlations of MSI, dMMR, and clinicopathological characteristics are summarised in Table 1. The mean age of all 580 patients was 55.6 years (range 24−86), and 385 (66.4%) patients were male. Epstein−Barr encoding region (EBER) *in situ* hybridisation was performed in 569 cases and EBV was positive in 25 cases (4.4%). In Lauren classification, there were 271 (46.7%) diffuse type GCs and 246 (42.4%) intestinal type GCs. There were 11 (1.9%) stage I cancers, 119 (20.5%) stage II cancers, 235 (40.5%) stage III cancers, and 215 (37.1%) stage IV cancers. The mean follow-up duration was 43.6 ± 35.0 months. Of 580 patients, 304 (52.4%) died during the follow up period, and the 5-year survival rate was 36.7%.

In all cases, IHC was performed in representative whole blocks using MLH1 (M1; Ventana, USA) with a BenchMark XT autostainer (Ventana), and MSH2 (G219-1129, 1:500; Cell Marque, USA), PMS2 (MRQ-28, 1:20; Cell Marque), and MSH6 (44/MSH6, 1:500; BD Biosciences, USA) with a Bond-Max autoimmunostainer (Leica Biosystems, Australia). Expression was reported as MMR proficient (pMMR; strong to weak nuclear staining with positive internal controls) or MMR deficient [dMMR; unequivocal loss of nuclear staining or focal (<20%) weak equivocal nuclear staining in the viable tumour cells in the presence of internal positive controls]. For MSI PCR testing, multiplex PCR was performed with five quasi-monomorphic mononucleotide repeat markers in all cases, as previously described.[3,6] Samples with allelic size variation in fewer than two microsatellites were classified as microsatellite-stable (MSS) and allelic size variations in two or more microsatellite markers were considered MSI-H. For cases with discrepant results between IHC and PCR tests, both experiments were repeated three times and the consistent results were used for final analyses.

For statistical analyses, we used age, sex, histological type by Lauren classification, World Health Organization (WHO) tumour classification, TNM stage (AJCC 8th edition), and overall survival (OS) of patients as clinical variables with the SPSS 24.0 statistical software program (IBM, USA). MSI/dMMR and clinicopathological variables were compared using Pearson's chi square test and were further analysed with linear-by-linear association. The Kaplan−Meier method was used to estimate OS. p values less than 0.05 were considered statistically significant.

MSI-H was found in 60 cases (10.3%) and dMMR was observed in 61 cases (10.5%) out of 580 GC (Fig. 1). All EBV-positive GC was pMMR and MSS. Both dMMR and MSI-H were significantly correlated with old age ($p<0.001$), low AJCC stage ($p<0.003$), intestinal-type by Lauren classification ($p<0.005$), and longer OS ($p<0.001$) (Table 1, Fig. 2). In multivariate analyses, dMMR and MSI-H were independent favourable prognostic factors ($p = 0.001$) in addition to AJCC stage (Supplementary Table 1, Appendix A).

In MMR IHC, 61 dMMR cases consisted of 52 MLH1/PMS2 losses (85.2%), four MSH2/MSH6 losses (6.6%), and

Table 1 The correlation of mismatch repair protein expression, microsatellite instability, and clinicopathological characteristics in 580 gastric cancer patients

	MLH1/PMS2		*p* value	MSH2/MSH6		*p* value	MMR protein		*p* value	Total	MSI		*p* value
	Preserved N=523	Loss N=57		Preserved N=571	Loss N=9		Proficient N=519	Deficient N=61			MSS N=520	MSI-H N=60	
Age													
≤60	338 (64.6)	19 (33.3)	<0.001	352 (61.6)	5 (55.6)	0.709	336 (64.7)	21 (34.4)	<0.001	357	337 (64.8)	20 (33.3)	<0.001
>60	185 (35.4)	38 (66.7)		219 (38.4)	4 (44.4)		183 (35.3)	40 (65.6)		223	183 (35.2)	40 (66.7)	
Sex													
Male	353 (67.5)	32 (56.1)	0.085	380 (66.5)	5 (55.6)	0.488	350 (67.4)	35 (57.4)	0.116	385	350 (67.3)	35 (58.3)	0.164
Female	170 (32.5)	25 (43.9)		191 (33.5)	4 (44.4)		169 (32.6)	26 (42.6)		195	170 (32.7)	25 (41.7)	
Lauren													
Intestinal	212 (40.5)	34 (59.6)	0.009	240 (42.0)	6 (66.7)	0.455	209 (40.3)	37 (60.7)	0.005	246	209 (40.2)	37 (61.7)	0.003
Mixed	32 (6.1)	6 (10.5)		38 (6.7)	0 (0.0)		32 (6.2)	6 (9.8)		38	32 (6.2)	6 (10.0)	
Diffuse	255 (48.8)	16 (28.1)		268 (46.9)	3 (33.3)		254 (48.9)	17 (27.9)		271	255 (49.0)	16 (26.7)	
Indeterminate	24 (4.6)	1 (1.8)		25 (4.4)	0 (0.0)		24 (4.6)	1 (1.6)		25	24 (4.6)	1 (1.7)	
Histology													
Tubular WD	9 (1.7)	0 (0.0)	<0.001	9 (1.6)	0 (0.0)	0.942	9 (1.7)	0 (0.0)	<0.001	9	9 (1.7)	0 (0.0)	<0.001
Tubular MD	151 (28.9)	25 (43.9)		171 (29.9)	5 (55.6)		148 (28.5)	28 (45.9)		176	148 (28.5)	28 (46.7)	
Tubular PD	114 (21.8)	24 (42.1)		136 (23.8)	2 (22.2)		114 (22.0)	24 (39.3)		138	114 (21.9)	24 (40.0)	
SRCC	179 (34.2)	4 (7.0)		181 (31.7)	2 (22.2)		178 (34.3)	5 (8.2)		183	179 (34.4)	4 (6.7)	
Mucinous	19 (3.6)	1 (1.8)		20 (3.5)	0 (0.0)		19 (3.7)	1 (1.6)		20	19 (3.7)	1 (1.7)	
Papillary	32 (6.1)	2 (3.5)		34 (6.0)	0 (0.0)		32 (6.2)	2 (3.3)		34	32 (6.2)	2 (3.3)	
Adenosquamous	0 (0.0)	1 (1.8)		1 (0.2)	0 (0.0)		0 (0.0)	1 (1.6)		1	0 (0.0)	1 (1.7)	
Undifferentiated	5 (1.0)	0 (0.0)		5 (0.9)	0 (0.0)		5 (1.0)	0 (0.0)		5	5 (1.0)	0 (0.0)	
Hepatoid	1 (0.2)	0 (0.0)		1 (0.2)	0 (0.0)		1 (0.2)	0 (0.0)		1	1 (0.2)	0 (0.0)	
Others	13 (2.5)	0 (0.0)		13 (2.3)	0 (0.0)		13 (2.5)	0 (0.0)		13	13 (2.5)	0 (0.0)	
TNM													
I	11 (2.1)	0 (0.0)	0.004[a]	10 (1.8)	1 (11.1)	0.185[a]	10 (1.9)	1 (1.6)	0.001[a]	11	10 (1.9)	1 (1.7)	0.003[a]
II	94 (18.0)	25 (43.9)		116 (20.3)	3 (33.3)		93 (17.9)	26 (42.6)		119	94 (18.1)	25 (41.7)	
III	219 (41.9)	16 (28.1)		233 (40.8)	2 (22.2)		218 (42.0)	17 (27.9)		235	218 (41.9)	17 (28.3)	
IV	199 (38.0)	16 (28.1)		212 (37.1)	3 (33.3)		198 (38.2)	17 (27.9)		215	198 (38.1)	17 (28.3)	
MSI													
MSS	519 (99.2)	1 (1.8)	<0.001	520 (91.1)	0 (0.0)	<0.001	519 (100)	1 (1.6)	<0.001	520			
MSI-H	4 (0.8)	56 (98.2)		51 (8.9)	9 (100)		0 (0.0)	60 (98.4)		60			

MD, moderately differentiated; MMR, mismatch repair gene; MSI, microsatellite instability; MSI-H, microsatellite instability-high; MSS, microsatellite stable; PD, poorly differentiated; SRCC, signet ring cell carcinoma; WD, well differentiated.
[a] Linear-to-linear association.

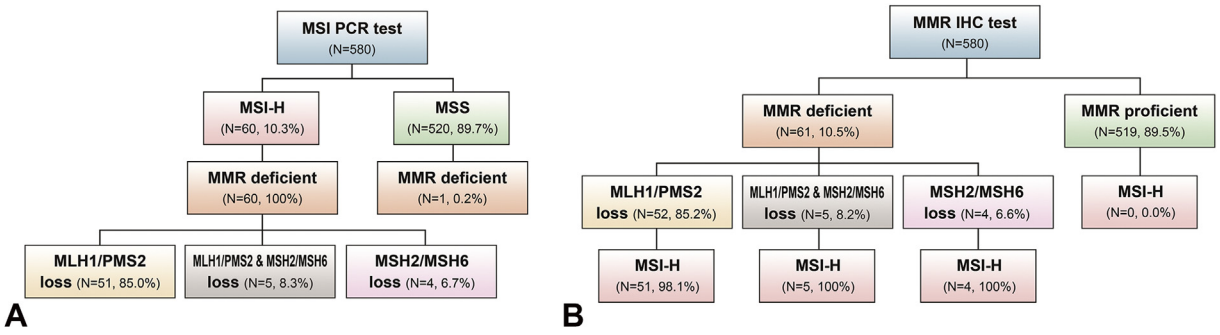

Fig. 1 The algorithms according to the order of execution of MSI PCR test and MMR IHC test. (A) MSI PCR was performed first, followed by MMR IHC. (B) MMR IHC was performed first and then MSI PCR was performed. IHC, immunohistochemistry; MMR, mismatch repair gene; MSI, microsatellite instability; MSI-H, microsatellite instability-high; MSS, microsatellite stable; PCR, polymerase chain reaction.

five MLH1/PMS2/MSH2/MSH6 losses (8.2%). Of 52 cases with MLH1/PMS2 losses, MSI-H was found in 51 cases (98.1%). All four cases with MSH2/MSH6 losses and five cases with MLH1/PMS2/MSH2/MSH6 losses were confirmed as MSI-H. In total, 60 of 61 dMMR GC with either MLH1/PMS2 or MSH2/MSH6 losses were confirmed to be MSI-H. The positive predictive value of dMMR for MSI-H was 98.4% (60/61). Among 519 MMR-proficient cases, PCR showed MSS in all cases and negative predictive value was 100% (519/519). The sensitivity and specificity of MMR protein IHC for MSI testing were 100% (60/60) and 99.8% (519/520), respectively.

We interpreted MMR IHC as unequivocal loss or focal (<20%) weak equivocal nuclear staining in viable tumour nuclei and we found only one (0.2%) case with discrepant results between MSI and MMR IHC. This patient was a 40-year-old female patient and showed 90% loss of MLH1 and 100% loss of PMS2 in IHC and multiplex PCR showed MSS (Supplementary Fig. 1, Appendix A). The patient's GC tumour was stage II poorly differentiated tubular adenocarcinoma and she was still alive without disease after 48.8 months of follow up. However, when we used focal weak equivocal nuclear staining in more than 20% of tumour cells for interpretation of dMMR, we found five discrepant cases

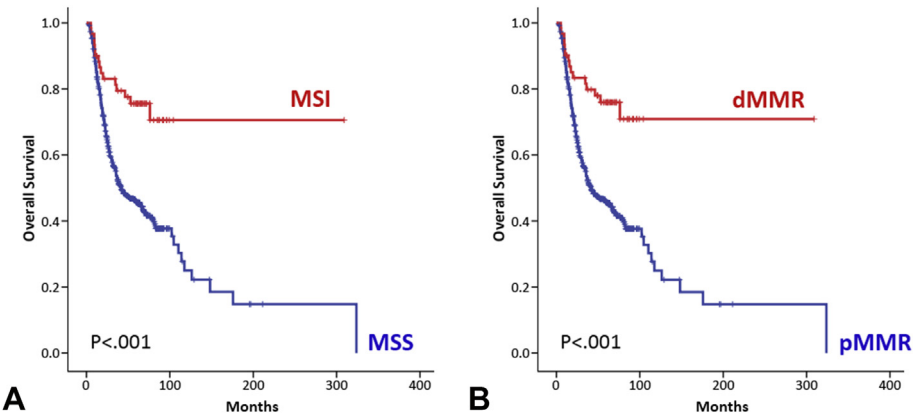

Fig. 2 The Kaplan–Meier curves of overall survival. (A) MSI and (B) dMMR GC were significantly associated with longer overall survival. dMMR, mismatch repair deficient; GC, gastric cancer; MSI, microsatellite instability; MSS, microsatellite stability; pMMR, mismatch repair proficient.

and the specificity (99.0%) was decreased. The clinicopathological characteristics of the remaining four patients with focal MMR losses are described in Supplementary Table 2 (Appendix A). Those patients with GC and focal MMR losses were confirmed as MSS and three of them showed distant metastasis after surgery and died of disease.

Immunotherapy is a promising cancer therapeutic modality that has recently emerged. MSI-H is a biomarker for anti-PD-1/PD-L1 inhibitors in GC. Clinical trials using pembrolizumab have also been underway in GC.[7] Therefore, diagnosing MSI is very important to establish a precise therapeutic strategy in patients with relapsed or refractory metastatic GC. Depending on the selection of MSI markers, the frequencies of MSI-H and dMMR GC vary and there has been no standardised MSI test algorithm that can replace PCR in GC.

Defects in the DNA MMR proteins result in a phenotype called MSI-H. The prevalence of MSI-H GC has ranged from 0% to 44.5%.[8] The difference in overall prevalence of MSI is related to patient cohort, methods used to detect MSI, and use of tissue microarrays for dMMR screening.[9] In this study of 580 GC cases with their representative whole block, the prevalence of MSI-H was 10.3%, and dMMR was found in 10.5% of cases, which is very similar to recent studies using both MMR IHC and the same PCR testing.[10]

Intriguingly, we found five MSI-H GC cases with concomitant losses of MLH1/PMS2/MSH2/MSH6 proteins and none of 580 cases showed a single MMR protein loss. For MSI-H in GC, direct comparison with dMMR is not well studied. In a previous large Korean cohort study in 464 GC cases with direct comparison of MSI and MLH1/MSH2 IHC, MLH1 loss was found in 88.2% and MSH2 in 7.4% and they also found co-losses of MLH1 and MSH2 in 4.4% of cases.[10] In MSI-GC, it is reported that about ~90% of cases are associated with MLH1/PMS2 losses. However, depending on microsatellite markers for MSI test, the frequencies of MSH2/MSH6 loss varied from 0% to 37%.[8] In the present study with four MMR proteins, we found MLH1/PMS2 losses in 85.2%, MSH2/MSH6 losses in 8.3% and co-losses of MLH1/PMS2/MSH2/MSH6 in 6.7% of MSI-H GC tumours, and the overall prevalence is similar to the previous observations.[10]

In MMR protein IHC for MSI testing in GC, the sensitivity was 100% and the specificity was 99.8%. This high concordance would be due to strict interpretation criteria to define dMMR (complete or >80% loss of expression). However, when we interpret focal losses of MMR as dMMR, the specificity was decreased although sensitivity was the same. In a previous study using two MMR proteins (MLH1 and MSH2), discordant results were found in 4.7% of cases.[10] Use of two more additional antibodies (PMS2 and MSH6) might have worked to increase the sensitivity and specificity because MMR IHC staining varied due to the sensitivities of primary antibodies and age of the paraffin blocks. So, for screening of MSI-H in GC, use of four antibodies is recommended to increase the accuracy to predict MSI.

In the present study, we found focal (<20%) losses of MMR in four MSS GC patients and three of them showed distant metastasis shortly after surgery and died of disease. Although we failed to find heterogeneous MSI-H in the present study, focal losses of MMR are interesting findings and warrant further studies exploring the mechanisms underlying focal MMR protein inactivation. Recently, we[11] and Mathiak *et al.*[9] found focal losses of MMR proteins and intratumoural heterogeneity in MSI-H patients with advanced stage GC. Given recently reported intratumoural heterogeneity in MSI-H GC and subsequent non-responsiveness for immune checkpoint inhibitors,[11] strict criteria for dMMR are recommended and further clinical correlation studies are recommended to support our hypothesis.

Conflicts of interest and sources of funding: This research was supported by grant (NRF-2017R1A2B4012436) from the National Research Foundation of Korea (NRF). The authors state that there are no conflicts of interest to disclose.

APPENDIX A. SUPPLEMENTARY DATA

Supplementary data to this article can be found online at https://doi.org/10.1016/j.pathol.2018.09.057.

Junhun Cho*, So Young Kang*, Kyoung-Mee Kim

*Department of Pathology and Translational Genomics, Samsung Medical Center, Sungkyunkwan University School of Medicine, Seoul, South Korea; *these authors contributed equally to the work presented here*

Contact Kyoung-Mee Kim.
E-mail: kkmkys@skku.edu

1. Cho J, Lee J, Bang H, *et al*. Programmed cell death-ligand 1 expression predicts survival in patients with gastric carcinoma with microsatellite instability. *Oncotarget* 2017; 8: 13320−8.
2. Cancer Genome Atlas Research Network. Comprehensive molecular characterization of gastric adenocarcinoma. *Nature* 2014; 513: 202−9.
3. Cristescu R, Lee J, Nebozhyn M, *et al*. Molecular analysis of gastric cancer identifies subtypes associated with distinct clinical outcomes. *Nat Med* 2015; 21: 449−56.
4. Ma C, Patel K, Singhi AD, *et al*. Programmed death-ligand 1 expression is common in gastric cancer associated with Epstein-Barr virus or microsatellite instability. *Am J Surg Pathol* 2016; 40: 1496−506.
5. An JY, Kim H, Cheong JH, *et al*. Microsatellite instability in sporadic gastric cancer: its prognostic role and guidance for 5-FU based chemotherapy after R0 resection. *Int J Cancer* 2012; 131: 505−11.
6. Min BH, Tae CH, Ahn SM, *et al*. Epstein-Barr virus infection serves as an independent predictor of survival in patients with lymphoepithelioma-like gastric carcinoma. *Gastric Cancer* 2016; 19: 852−9.
7. Muro K, Chung HC, Shankaran V, *et al*. Pembrolizumab for patients with PD-L1-positive advanced gastric cancer (KEYNOTE-012): a multicentre, open-label, phase 1b trial. *Lancet Oncol* 2016; 17: 717−26.
8. Lee J, Kim K-M. Biomarkers for gastric cancer: molecular classification revisited. *Precis Future Med* 2017; 1: 59−68.
9. Mathiak M, Warneke VS, Behrens HM, *et al*. Clinicopathologic characteristics of microsatellite instable gastric carcinomas revisited: urgent need for standardization. *Appl Immunohistochem Mol Morphol* 2017; 25: 12−24.
10. Bae YS, Kim H, Noh SH, *et al*. Usefulness of immunohistochemistry for microsatellite instability screening in gastric cancer. *Gut Liver* 2015; 9: 629−35.
11. Kim ST, Cristescu R, Bass AJ, *et al*. Comprehensive molecular characterization of clinical responses to PD-1 inhibition in metastatic gastric cancer. *Nat Med* 2018; 24: 1449−58.

DOI: https://doi.org/10.1016/j.pathol.2018.09.057

Maternally expressed, paternally imprinted, embryonic non-coding RNA are expressed in osteosarcoma, Ewing sarcoma and spindle cell sarcoma

Sir,

In a human embryo it takes 8 weeks after fertilisation for the skeleton to begin to form, one of the last organs to develop before becoming a foetus. Mesenchymal progenitors, derived from neural crest cells, differentiate into chondrocytes where the skeleton is generated as a mostly cartilage template. Other mesenchymal progenitors envelop the template, activate runt related transcription factor 2 (RUNX2) and bone morphogenetic protein 2 (BMP2) and differentiate into osteoblasts, where an osteoid matrix is secreted and subsequently mineralised to become bone.[1] During development and up to late adolescence, cellular proliferation enabling skeletal growth is restricted to the metaphysis and epiphyseal line or 'growth plate'. It is in the growth plate of long bones where most bone cancers develop, hence the predominantly childhood incidence of the cancer. Primitive mesenchymal cells undergo transformation to form a heterogeneous group of bone malignancies. The most common type of bone cancer in children is osteosarcoma, mostly initiated by tumour protein p53 (*TP53*) structural variants. The second most common type of bone cancer in children is Ewing sarcoma, mostly initiated by a EWS RNA binding protein 1-Fli-1 proto-oncogene, ETS transcription factor (*EWSR1-FLI1*) fusion. There are an average of 160 and 55 new cases of osteosarcoma and Ewing sarcoma, respectively, every year in the UK. Five-year survival for both cancer types is 50% when diagnosed early. Five-year survival is 15% when lung metastases are present at diagnosis. Treatment progress for bone cancer is poor when compared to other cancers such as breast where there is a 20 year survival of 70%. Bone cancer requires extensive and sometimes disabling multimodal treatment. Chemotherapy for osteosarcoma includes methotrexate, cisplatin and doxorubicin, which were developed in the 1940s and 1970s. Chemotherapy for Ewing sarcoma includes vincristine, ifosfamide and etoposide, which were developed in the 1960s and 1980s. If the tumour responds well to chemotherapy and radiotherapy, wide area resection or amputation is performed. New understanding of bone cancer biology leading to better diagnosis and better treatments is required.

Transcriptomic analysis of bone cancer is lacking. Different RNA populations within cells are generally classified as coding and non-coding, i.e., whether they have protein coding potential. Messenger RNA (mRNA) molecules contain a start codon 'AUG' encoding methionine at the beginning of an open reading frame. Non-coding RNA lack protein coding ability and usually exist within the cell without a start codon. Over 70% of known non-coding RNA are long non-coding RNA (lncRNA) that are classed by their >200 nucleotide (nt) length. Similarly to mRNA, lncRNA are transcribed by RNA polymerase II, have a 5′ cap and are polyadenylated. LncRNAs have a large diversity of roles including regulation of chromatin dynamics, enforcing imprinting and as microRNA inhibitors by acting as a microRNA 'sponge'. LncRNAs are further classified based on their genomic localisation. Intergenic lncRNAs are named for their production from loci in between genes. Intronic lncRNAs are named for their production from mRNA introns. Sense lncRNAs are named for their production from the sense strand of protein coding genes that overlap with an exon/intron. Antisense lncRNAs are named for their production from the antisense strand of protein coding genes that overlap with an exon/intron. Another elusive class of non-coding RNA is the small nucleolar RNAs (snoRNAs). SnoRNAs are 60−170 nt in length and are classed as C/D box snoRNAs and H/ACA box snoRNAs. C/D box snoRNAs guide 2′-O-methylation of ribosomal and transfer RNA. H/ACA box snoRNAs guide pseudouridylation mostly in transfer RNAs. The majority of snoRNA are intronic. There is a recent interest in lncRNA and snoRNA and their role in cancer biology. We took a next generation sequencing and bioinformatics approach to evaluate lncRNA and snoRNA expression in bone cancer.

We extracted RNA using the miRCURY RNA isolation kit (Exiqon, Denmark) from two tissue specimens of osteoblastic osteosarcoma (patient ages 15 and 19, OS1 and OS2, respectively). OS1 had undergone treatment with cisplatin and doxorubicin prior to surgery (Fig. 1A,B). OS2 had undergone treatment with methotrexate, cisplatin and doxorubicin prior to surgery (Fig. 1C,D). We extracted RNA from one tissue specimen of Ewing sarcoma (patient age 6, ES) where the patient had undergone nine alternating cycles of vincristine, doxorubicin and cyclophosphamide in one cycle and ifosfamide and etoposide in another cycle prior to surgery (Fig. 1E,F). We extracted RNA from one tissue specimen of a spindle cell sarcoma of bone (patient age 17, SCS) where the patient had not undergone systemic treatment (Fig. 1G,H). We used publicly available data for four control samples, which were obtained from long bone tissue derived from surgical